Imperfections in Crystals

Course code: 053313 PHY 3107
Course title: Solid State Physics I
Bachelor of Science with Honours in Physics
Jashore University of Science and Technology

Content

Classification of Defects; Point Defects; Dislocations Screw and Edge Dislocations; Diffusion in Metals; Plane Defects; Crystal Grains and Grain Boundaries; Energy of Grain Boundaries; Color Centers.

References

Introduction to Solid State Physics – Charles Kittel
Solid State Physics – Neil W. Ashcroft, N. David Mermin
Elementary Solid State Physics: Principles and Applications – M. Ali Omar

20
Point Defects

LATTICE VACANCIES 585

DIFFUSION 588
- **Metals** 591

COLOR CENTERS 592
- ***F* centers** 592
- **Other centers in alkali halides** 593

PROBLEMS 595

1. **Frenkel defects** 595
2. **Schottky vacancies** 595
3. ***F* center** 595

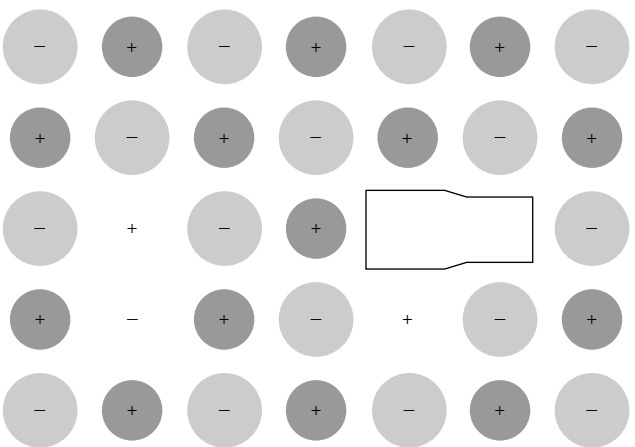


Figure 1 A plane of a pure alkali halide crystal, showing two vacant positive ion sites, and a coupled pair of vacant sites of opposite sign.

The common point imperfections in crystals are chemical impurities, vacant lattice sites, and extra atoms not in regular lattice positions. Linear imperfections are treated under dislocations, Chapter 21. The crystal surface is a planar imperfection, with electron, phonon, and magnon surface states.

Some important properties of crystals are controlled as much by imperfections as by the composition of the host crystal, which may act only as a solvent or matrix or vehicle for the imperfections. The conductivity of some semiconductors is due entirely to trace amounts of chemical impurities. The color and luminescence of many crystals arise from impurities or imperfections. Atomic diffusion may be accelerated enormously by impurities or imperfections. Mechanical and plastic properties are usually controlled by imperfections.

LATTICE VACANCIES

The simplest imperfection is a **lattice vacancy**, which is a missing atom or ion, also known as a **Schottky defect**. (Fig. 1). We create a Schottky defect in a perfect crystal by transferring an atom from a lattice site in the interior to a lattice site on the surface of the crystal. In thermal equilibrium a certain number of lattice vacancies are always present in an otherwise perfect crystal, because the entropy is increased by the presence of disorder in the structure.

In metals with close-packed structures the proportion of lattice sites vacant at temperatures just below the melting point is of the order of 10^{-3} to 10^{-4}. But in some alloys, in particular the very hard transition metal carbides such as TiC, the proportion of vacant sites of one component can be as high as 50 percent.

The probability that a given site is vacant is proportional to the Boltzmann factor for thermal equilibrium: $P = \exp(-E_V/k_BT)$, where E_V is the energy required to take an atom from a lattice site inside the crystal to a lattice site on the surface. If there are N atoms, the equilibrium number n of vacancies is given by the Boltzmann factor

$$\frac{n}{N-n} = \exp(-E_V/k_BT) \ . \tag{1}$$

If $n \ll N$, then

$$n/N \cong \exp(-E_V/k_BT) \ . \tag{2}$$

If $E_V \approx 1$ eV and $T \approx 1000$ K, then $n/N \approx e^{-12} \approx 10^{-5}$.

The equilibrium concentration of vacancies decreases as the temperature decreases. The actual concentration of vacancies will be higher than the

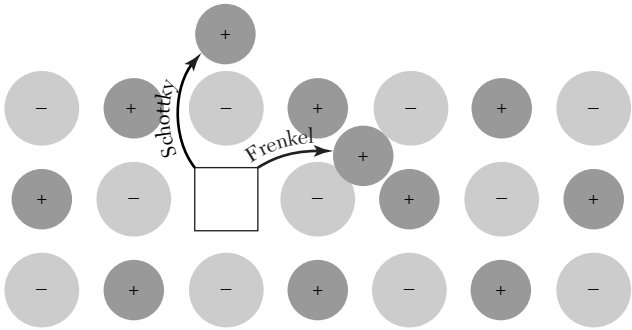


Figure 2 Schottky and Frenkel defects in an ionic crystal. The arrows indicate the displacement of the ions. In a Schottky defect the ion ends up on the surface of the crystal; in a Frenkel defect the ion is removed to an interstitial position.

equilibrium value if the crystal is grown at an elevated temperature and then cooled suddenly, thereby freezing in the vacancies (see the discussion of diffusion below).

In ionic crystals it is usually energetically favorable to form roughly equal numbers of positive and negative ion vacancies. The formation of pairs of vacancies keeps the crystal electrostatically neutral on a local scale. From a statistical calculation we obtain

$$n \cong N \exp(-E_p/2k_BT) \tag{3}$$

for the number of pairs, where E_p is the energy of formation of a pair.

Another vacancy defect is the **Frenkel defect** (Fig. 2) in which an atom is transferred from a lattice site to an **interstitial position**, a position not normally occupied by an atom. In pure alkali halides the most common lattice vacancies are Schottky defects; in pure silver halides the most common vacancies are Frenkel defects. The calculation of the equilibrium number of Frenkel defects proceeds along the lines of Problem 1. If the number n of Frenkel defects is much smaller than the number of lattice sites N and the number of interstitial sites N', the result is

$$n \cong (NN')^{1/2} \exp(-E_I/2k_BT) \ , \tag{4}$$

where E_I is the energy necessary to remove an atom from a lattice site to an interstitial position.

Lattice vacancies are present in alkali halides when these contain additions of divalent elements. If a crystal of KCl is grown with controlled amounts of $CaCl_2$, the density varies as if a K^+ lattice vacancy were formed for each Ca^{2+} ion in the crystal. The Ca^{2+} enters the lattice in a normal K^+ site and the two Cl^- ions enter two Cl^- sites in the KCl crystal (Fig. 3). Demands of charge neutrality result in a vacant metal ion site. The experimental results show that the addition of $CaCl_2$ to KCl lowers the density of the crystal. The density

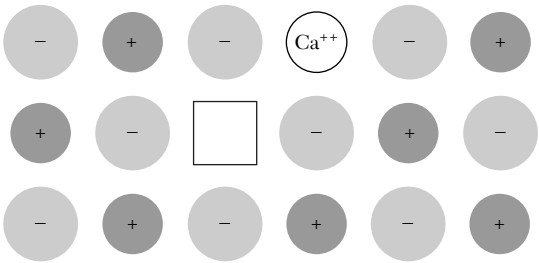


Figure 3 Production of a lattice vacancy by the solution of $CaCl_2$ in KCl: to ensure electrical neutrality, a positive ion vacancy is introduced into the lattice with each divalent cation Ca^{++}. The two Cl^- ions of $CaCl_2$ enter normal negative ion sites.

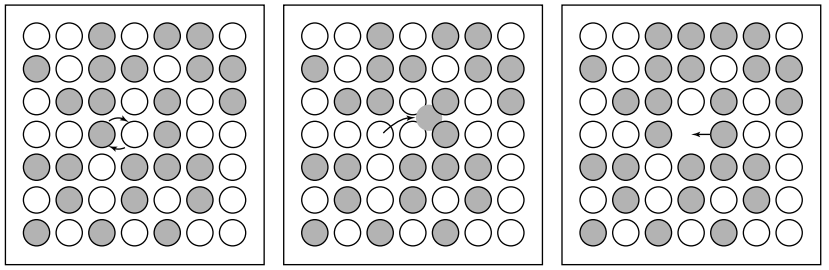


Figure 4 Three basic mechanisms of diffusion: (a) Interchange by rotation about a midpoint. More than two atoms may rotate together. (b) Migration through interstitial sites. (c) Atoms exchange position with vacant lattice sites. (After Seitz.)

would increase if no vacancies were produced, because Ca^{2+} is a heavier and smaller ion than K^+.

The mechanism of electrical conductivity in alkali and silver halide crystals is usually by the motion of ions and not by the motion of electrons. This has been established by comparing the transport of charge with the transport of mass as measured by the material plated out on electrodes in contact with the crystal.

The study of ionic conductivity is an important tool in the investigation of lattice defects. Work on alkali and silver halides containing known additions of divalent metal ions shows that at not too high temperatures the ionic conductivity is directly proportional to the amount of divalent addition. This is not because the divalent ions are intrinsically highly mobile, for it is predominantly the monovalent metal ion which deposits at the cathode. The lattice vacancies introduced with the divalent ions are responsible for the enhanced diffusion (Fig. 4c). The diffusion of a vacancy in one direction is equivalent to the diffusion of an atom in the opposite direction. When lattice defects are generated thermally, their energy of formation gives an extra contribution to the heat capacity of the crystal, as shown in Fig. 5.

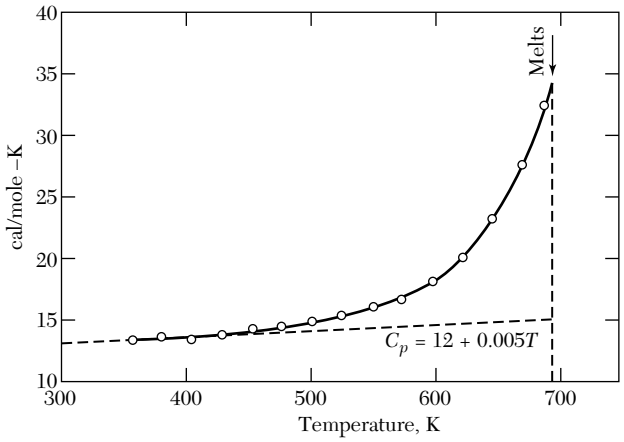


Figure 5 Heat capacity of silver bromide exhibiting the excess heat capacity from the formation of lattice defects. (After R. W. Christy and A. W. Lawson.)

An associated pair of vacancies of opposite sign exhibits an electric dipole moment, with contributions to the dielectric constant and dielectric loss due to the motion of pairs of vacancies. The dielectric relaxation time is a measure of the time required for one of the vacant sites to jump by one atomic position with respect to the other. The dipole moment can change at low frequencies, but not at high. In sodium chloride the relaxation frequency is 1000 s^{-1} at 85°C.

DIFFUSION

When there is a concentration gradient of impurity atoms or vacancies in a solid, there will be a flux of these through the solid. In equilibrium the impurities or vacancies will be distributed uniformly. The net flux J_N of atoms of one species in a solid is related to the gradient of the concentration N of this species by a phenomenological relation called **Fick's law**:

$$\boldsymbol{J}_N = -D \operatorname{grad} N \ . \tag{5}$$

Here J_N is the number of atoms crossing unit area in unit time; the constant D is the **diffusion constant** or **diffusivity** and has the units cm^2/s or m^2/s. The minus sign means that diffusion occurs away from regions of high concentration. The form (5) of the law of diffusion is often adequate, but rigorously the gradient of the chemical potential is the driving force for diffusion and not the concentration gradient alone (*TP*, p. 406).

The diffusion constant is often found to vary with temperature as

$$D = D_0 \exp(-E/k_B T) \ ; \tag{6}$$

here E is the **activation energy** for the process. Experimental results on the diffusion of carbon in alpha iron are shown in Fig. 6. The data are represented

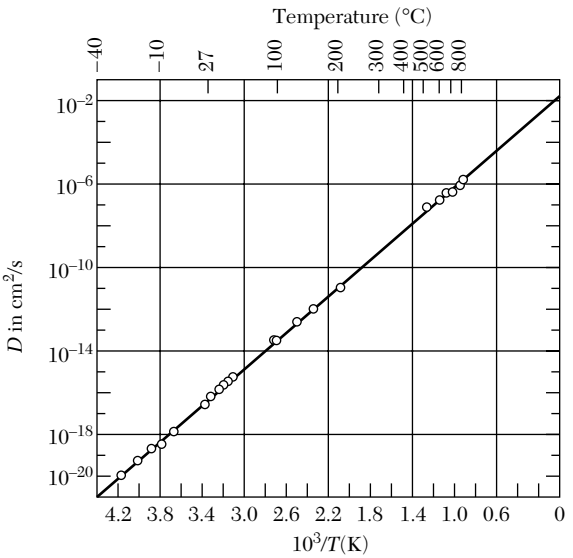


Figure 6 Diffusion coefficient of carbon in iron, after Wert. The logarithm of D is directly proportional to $1/T$.

Table 1 Diffusion constants and activation energies

Host crystal	Atom	D_0 $cm^2\ s^{-1}$	E eV	Host crystal	Atom	D_0 $cm^2\ s^{-1}$	E eV
Cu	Cu	0.20	2.04	Si	Al	8.0	3.47
Cu	Zn	0.34	1.98	Si	Ga	3.6	3.51
Ag	Ag	0.40	1.91	Si	In	16.0	3.90
Ag	Cu	1.2	2.00	Si	As	0.32	3.56
Ag	Au	0.26	1.98	Si	Sb	5.6	3.94
Ag	Pb	0.22	1.65	Si	Li	2×10^{-3}	0.66
Na	Na	0.24	0.45	Si	Au	1×10^{-3}	1.13
U	U	2×10^{-3}	1.20	Ge	Ge	10.0	3.1

by $E = 0.87$ eV, $D_0 = 0.020$ cm^2/s. Representative values of D_0 and E are given in Table 1.

To diffuse, an atom must overcome the potential energy barrier presented by its nearest neighbors. We treat the diffusion of impurity atoms between interstitial sites. The same argument will apply to the diffusion of vacant lattice sites. If the barrier is of height E, the atom will have sufficient thermal energy to pass over the barrier a fraction $\exp(-E/k_BT)$ of the time. Quantum tunneling through the barrier is another possible process, but is usually important only for the lightest nuclei, particularly hydrogen.

If ν is a characteristic atomic vibrational frequency, then the probability p that during unit time the atom will have enough thermal energy to pass over the barrier is

$$p \approx \nu \exp(-E/k_B T) \ . \tag{7}$$

In unit time the atom makes ν passes at the barrier, with a probability $\exp(-E/k_B T)$ of surmounting the barrier on each try. The quantity p is called the *jump frequency.*

We consider two parallel planes of impurity atoms in interstitial sites. The planes are separated by lattice constant a. There are S impurity atoms on one plane and $(S + a\, dS/dx)$ on the other. The net number of atoms crossing between the planes in unit time is $\approx -pa\, dS/dx$. If N is the total concentration of impurity atoms, then $S = aN$ per unit area of a plane.

The diffusion flux may now be written as

$$J_N \approx -pa^2(dN/dx) \ . \tag{8}$$

On comparison with (5) we have the result

$$\boxed{D = \nu a^2 \exp(-E/k_B T) \ .} \tag{9}$$

of the form (6) with $D_0 = \nu a^2$.

If the impurities are charged, we may find the ionic mobility $\bar{\mu}$ and the conductivity σ from the diffusivity by using the Einstein relation $k_B T \bar{\mu} = qD$ from *TP*, p. 406:

$$\bar{\mu} = (q\nu a^2/k_B T) \exp(-E/k_B T) \ ; \tag{10}$$

$$\sigma = Nq\bar{\mu} = (Nq^2 \nu a^2/k_B T) \exp(-E/k_B T) \ , \tag{11}$$

where N is the concentration of impurity ions of charge q.

The proportion of vacancies is independent of temperature in the range in which the number of vacancies is determined by the number of divalent metal ions. Then the slope of a plot of $\ln \sigma$ versus $1/k_B T$ gives E_+, the barrier activation energy for the jumping of positive ion vacancies (Table 2). Diffusion is very slow at low temperatures. At room temperature the jump frequency is of the order of $1\,\mathrm{s}^{-1}$, and at 100 K it is of the order of $10^{-25}\ \mathrm{s}^{-1}$.

The proportion of vacancies in the temperature range in which the concentration of defects is determined by thermal generation is given by

$$f \cong \exp(-E_f/2k_B T) \ , \tag{12}$$

where E_f is the energy of formation of a vacancy pair, according to the theory of Schottky or Frenkel defects. Here the slope of a plot of $\ln \sigma$ versus $1/k_B T$ will be $E_+ + \frac{1}{2}E_f$, according to (10) and (12). From measurements in different

Table 2 Activation energy E_+ for motion of a positive ion vacancy

Values of the energy of formation of a vacancy pair, E_f, are also given. The numbers given in parentheses for the silver salts refer to interstitial silver ions.

Crystal	E_+(eV)	E_f(eV)	Workers
NaCl	0.86	2.02	Etzel and Maurer
LiF	0.65	2.68	Haven
LiCl	0.41	2.12	Haven
LiBr	0.31	1.80	Haven
LiI	0.38	1.34	Haven
KCl	0.89	2.1–2.4	Wagner; Kelting and Witt
AgCl	0.39(0.10)	1.4[a]	Teltow
AgBr	0.25(0.11)	1.1[a]	Compton

[a]For Frenkel defect.

temperature ranges we determine the energy of formation of a vacancy pair E_f and the jump activation energy E_+.

The diffusion constant can be measured by radioactive tracer techniques. The diffusion of a known initial distribution of radioactive ions is followed as a function of time or distance. Values of the diffusion constant thus determined may be compared with values from ionic conductivities. The two sets of values do not usually agree within the experimental accuracy, suggesting the presence of a diffusion mechanism that does not involve the transport of charge. For example, the diffusion of pairs of positive and negative ion vacancies does not involve the transport of charge.

Metals

Self-diffusion in monatomic metals most commonly proceeds by lattice vacancies. **Self-diffusion** means the diffusion of atoms of the metal itself, and not of impurities. The activation energy for self-diffusion in copper is expected to be in the range 2.4 to 2.7 eV for diffusion through vacancies and 5.1 to 6.4 eV for diffusion through interstitial sites. Observed values of the activation energy are 1.7 to 2.1 eV.

Activation energies for diffusion in Li and Na can be determined from measurements of the temperature dependence of the nuclear resonance line width. As discussed under magnetic resonance, the resonance line width narrows when the jump frequency of an atom between sites becomes rapid in comparison with the frequency corresponding to the static line width. The values 0.57 eV and 0.45 eV were determined by NMR for Li and Na. Self-diffusion measurements for sodium also give 0.4 eV.

COLOR CENTERS

Pure alkali halide crystals are transparent throughout the visible region of the spectrum. A **color center** is a lattice defect that absorbs visible light. An ordinary lattice vacancy does not color alkali halide crystals, although it affects the absorption in the ultraviolet. The crystals may be colored in a number of ways:

- by the introduction of chemical impurities;
- by the introduction of an excess of the metal ion (we may heat the crystal in the vapor of the alkali metal and then cool it quickly—an NaCl crystal heated in the presence of sodium vapor becomes yellow; a KCl crystal heated in potassium vapor becomes magenta);
- by x-ray, γ-ray, neutron, and electron bombardment; and
- by electrolysis.

F Centers

The name *F* center comes from the German word for color, *Farbe*. We usually produce *F* centers by heating the crystal in excess alkali vapor or by x-irradiation. The central absorption band (*F* band) associated with *F* centers in several alkali halides are shown in Fig. 7, and the quantum energies are listed in Table 3. Experimental properties of *F* centers have been investigated in detail, originally by Pohl.

The *F* center has been identified by electron spin resonance as an electron bound at a negative ion vacancy (Fig. 8), in agreement with a model suggested by de Boer. When excess alkali atoms are added to an alkali halide crystal, a corresponding number of negative ion vacancies are created. The valence electron of the alkali atom is not bound to the atom; the electron migrates in the crystal and becomes bound to a vacant negative ion site. A negative ion vacancy in a perfect periodic lattice has the effect of an isolated positive charge: it attracts and binds an electron. We can simulate the electrostatic effect of

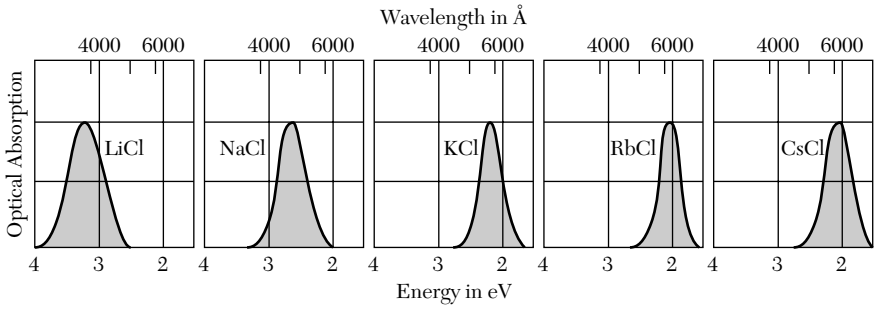


Figure 7 The *F* bands for several alkali halides: optical absorption versus wavelength for crystals that contain *F* centers.

Table 3 Experimental *F* center absorption energies, in eV

LiCl	3.1	NaBr	2.3
NaCl	2.7	KBr	2.0
KCl	2.2	RbBr	1.8
RbCl	2.0	LiF	5.0
CsCl	2.0	NaF	3.6
LiBr	2.7	KF	2.7

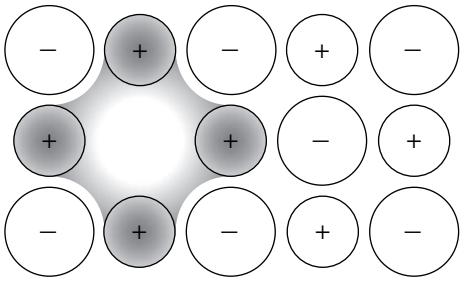


Figure 8 An *F* center is a negative ion vacancy with one excess electron bound at the vacancy. The distribution of the excess electron is largely on the positive metal ions adjacent to the vacant lattice site.

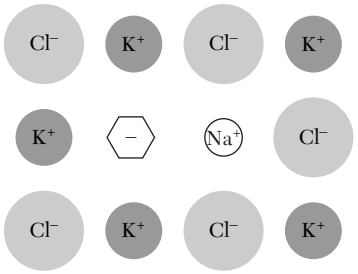


Figure 9 An F_A center in KCl: one of the six K^+ ions which bind an *F* center is replaced by another alkali ion, here Na^+.

a negative ion vacancy by adding a positive charge q to the normal charge $-q$ of an occupied negative ion site.

The *F* center is the simplest trapped-electron center in alkali halide crystals. The optical absorption of an *F* center arises from an electric dipole transition to a bound excited state of the center.

Other Centers in Alkali Halides

In the F_A center one of the six nearest neighbors of an *F* center has been replaced by a different alkali ion, Fig. 9. More complex trapped-electron centers are formed by groups of *F* centers, Fig. 10 and 11. Thus two adjacent *F* centers form an *M* center. Three adjacent *F* centers form an *R* center. Different centers are distinguished by their optical absorption frequencies.

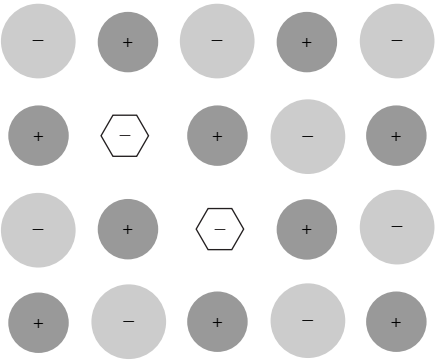


Figure 10 An M center consists of two adjacent F centers.

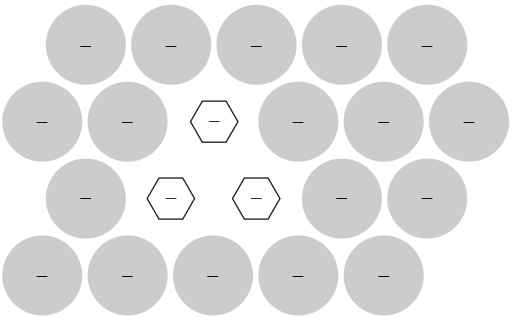


Figure 11 An R center consists of three adjacent F centers; that is, a group of three negative ion vacancies in a [111] plane of the NaCl structure, with three associated electrons.

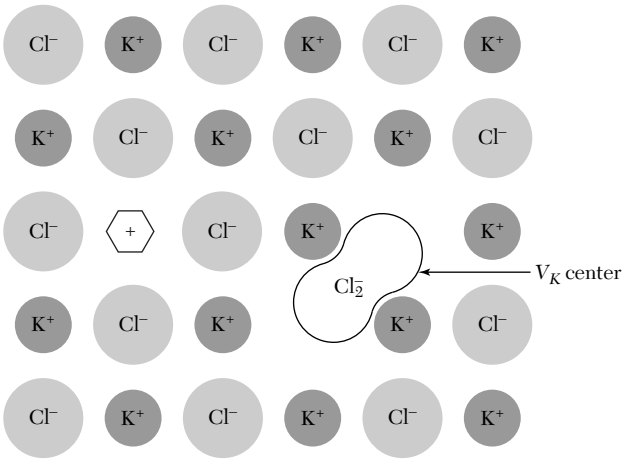


Figure 12 A V_K center formed when a hole is trapped by a pair of negative ions resembles a negative halogen molecule ion, which is Cl_2^- in KCl. No lattice vacancies or extra atoms are involved in a V_K center. The center at the left of the figure probably is not stable: the hexagon represents a hole trapped near a positive ion vacancy; such a center would be the antimorph to an F center. Holes have a lower energy trapped in a V_K center than in an anti-F center.

Holes may be trapped to form color centers, but hole centers are not usually as simple as electron centers. For example, a hole in the filled p^6 shell of a halogen ion leaves the ion in a p^5 configuration, whereas an electron added to the filled p^6 shell of an alkali ion leaves the ion in a p^6s configuration.

The chemistry of the two centers is different: p^6s acts as a spherically symmetric ion, but p^5 acts as an asymmetric ion and, by virtue of the Jahn-Teller effect, will distort its immediate surroundings in the crystal.

The antimorph to the F center is a hole trapped at a positive ion vacancy, but no such center has been identified experimentally in alkali halides; in insulating oxides the O^- (called V^-) defect is known. The best-known trapped-hole center is the V_K center, Fig. 12. The V_K center is formed when a hole is trapped by a halogen ion in an alkali halide crystal. Electron spin resonance shows that the center is like a negative halogen molecular ion, such as Cl_2^- in KCl. The Jahn-Teller trapping of free holes is the most effective form of self-trapping of charge carriers in perfect crystals.

Problems

1. ***Frenkel defects.*** Show that the number n of interstitial atoms in equilibrium with n lattice vacancies in a crystal having N lattice points and N' possible interstitial positions is given by the equation

$$E_I = k_B T \ln [(N - n)(N' - n)/n^2] \ ,$$

whence, for $n \ll N, N'$, we have $n \simeq (NN')^{1/2} \exp(-E_I/2k_BT)$. Here E_I is the energy necessary to remove an atom from a lattice site to an interstitial position.

2. ***Schottky vacancies.*** Suppose that the energy required to remove a sodium atom from the inside of a sodium crystal to the boundary is 1 eV. Calculate the concentration of Schottky vacancies at 300 K.

3. ***F center.*** (a) Treat an F center as a free electron of mass m moving in the field of a point charge e in a medium of dielectric constant $\epsilon = n^2$; what is the $1s$-$2p$ energy difference of F centers in NaCl? (b) Compare from Table 3 the F center excitation energy in NaCl with the $3s$-$3p$ energy difference of the free sodium atom.

21
Dislocations

SHEAR STRENGTH OF SINGLE CRYSTALS 599
- **Slip** 600

DISLOCATIONS 601
- **Burgers vectors** 604
- **Stress fields of dislocations** 605
- **Low-angle grain boundaries** 607
- **Dislocation densities** 610
- **Dislocation multiplication and slip** 611

STRENGTH OF ALLOYS 613

DISLOCATIONS AND CRYSTAL GROWTH 615
- **Whiskers** 616

HARDNESS OF MATERIALS 617

PROBLEMS 618

1. **Lines of closest packing** 618
2. **Dislocation pairs** 618
3. **Force on dislocation** 618

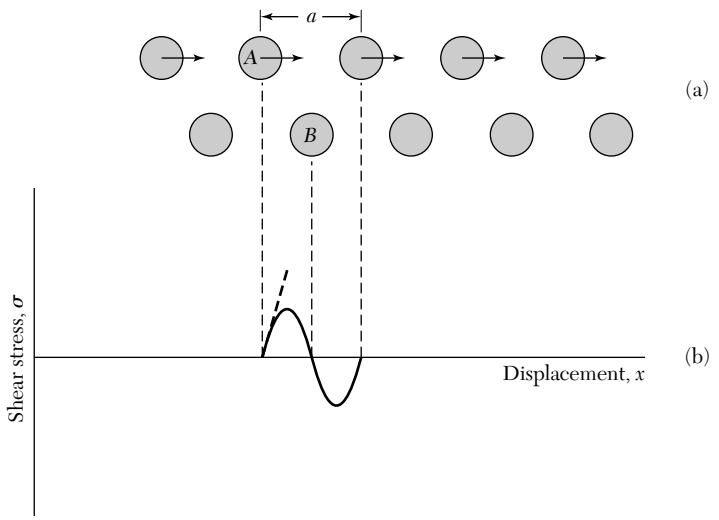


Figure 1 (a) Relative shear of two planes of atoms (shown in section) in a uniformly strained crystal; (b) shear stress as a function of the relative displacement of the planes from their equilibrium position. The heavy broken line drawn at the initial slope defines the shear modulus G.

This chapter is concerned with the interpretation of the plastic mechanical properties of crystalline solids in terms of the theory of dislocations. Plastic properties are irreversible deformations; elastic properties are reversible. The ease with which pure single crystals deform plastically is striking. This intrinsic weakness of crystals is exhibited in various ways. Pure silver chloride melts at 455°C, yet at room temperature it has a cheeselike consistency and can be rolled into sheets. Pure aluminum crystals are elastic (follow Hooke's law) only to a strain of about 10^{-5}, after which they deform plastically.

Theoretical estimates of the strain at the elastic limit of perfect crystals may give values 10^3 or 10^4 higher than the lowest observed values, although a factor 10^2 is more usual. There are few exceptions to the rule that pure crystals are plastic and are not strong: crystals of germanium and silicon are not plastic at room temperature and fail or yield only by fracture. Glass at room temperature fails only by fracture, but it is not crystalline. The fracture of glass is caused by stress concentration at minute cracks.

SHEAR STRENGTH OF SINGLE CRYSTALS

Frenkel gave a simple method of estimating the theoretical shear strength of a perfect crystal. We consider in Fig. 1 the force needed to make a shear displacement of two planes of atoms past each other. For small elastic strains, the stress σ is related to the displacement x by

$$\sigma = Gx/d \quad . \tag{1}$$

Here d is the interplanar spacing, and G denotes the appropriate shear modulus. When the displacement is large and has proceeded to the point that atom A is directly over atom B in the figure, the two planes of atoms are in a configuration of unstable equilibrium and the stress is zero. As a first approximation we represent the stress-displacement relation by

$$\sigma = (Ga/2\pi d) \sin (2\pi x/a) \quad , \tag{2}$$

where a is the interatomic spacing in the direction of shear. This relation is constructed to reduce to (1) for small values of x/a. The critical shear stress σ_c at which the lattice becomes unstable is given by the maximum value of σ, or

$$\sigma_c = Ga/2\pi d \quad . \tag{3}$$

If $a \approx d$, then $\sigma_c \approx G/2\pi$: the ideal critical shear stress is of the order of $\frac{1}{6}$ of the shear modulus.

Table 1 Comparison of shear modulus G and observed elastic limit σ_c[a]

	Shear modulus G, in dyn/cm^2	Elastic limit σ_c, in dyn/cm^2	G/σ_c
Sn, single crystal	1.9×10^{11}	1.3×10^{7}	15,000
Ag, single crystal	2.8×10^{11}	6×10^{6}	45,000
Al, single crystal	2.5×10^{11}	4×10^{6}	60,000
Al, pure, polycrystal	2.5×10^{11}	2.6×10^{8}	900
Al, commercial drawn	$\sim 2.5 \times 10^{11}$	9.9×10^{8}	250
Duralumin	$\sim 2.5 \times 10^{11}$	3.6×10^{9}	70
Fe, soft, polycrystal	7.7×10^{11}	1.5×10^{9}	500
Heat-treated carbon steel	$\sim 8 \times 10^{11}$	6.5×10^{9}	120
Nickel-chrome steel	$\sim 8 \times 10^{11}$	1.2×10^{10}	65

[a]After Mott.

The observations in Table 1 show the experimental values of the elastic limit are much smaller than (3) would suggest. The theoretical estimate may be improved by consideration of the actual form of the intermolecular forces and by consideration of other configurations of mechanical stability available to the lattice as it is sheared. Mackenzie has shown that these two effects may reduce the theoretical ideal shear strength to about $G/30$, corresponding to a critical shear strain angle of about 2 degrees. The observed low values of the shear strength can be explained only by the presence of imperfections that can act as sources of mechanical weakness in real crystals. The movement of crystal imperfections called dislocations is responsible for slip at very low applied stresses.

Slip

Plastic deformation in crystals occurs by slip, an example of which is shown in Fig. 2. In slip, one part of the crystal slides as a unit across an adjacent part. The surface on which slip takes place is known as the slip plane. The direction of motion is known as the slip direction. The great importance of lattice properties for plastic strain is indicated by the highly anisotropic nature of slip. Displacement takes place along crystallographic planes with a set of small Miller indices, such as the {111} planes in fcc metals and the {110}, {112}, and {123} planes in bcc metals.

The slip direction is in the line of closest atomic packing, ⟨110⟩ in fcc metals and ⟨111⟩ in bcc metals (Problem 1). To maintain the crystal structure after slip, the displacement or slip vector must equal a lattice translation vector. The shortest lattice translation vector expressed in terms of the lattice constant a in a fcc structure is of the form $(a/2)(\hat{\mathbf{x}} + \hat{\mathbf{y}})$; in a bcc structure it is $(a/2)(\hat{\mathbf{x}} + \hat{\mathbf{y}} + \hat{\mathbf{z}})$. But in fcc crystals one also observes partial displacements which upset the regular sequence *ABCABC* . . . of closest-packed planes, to

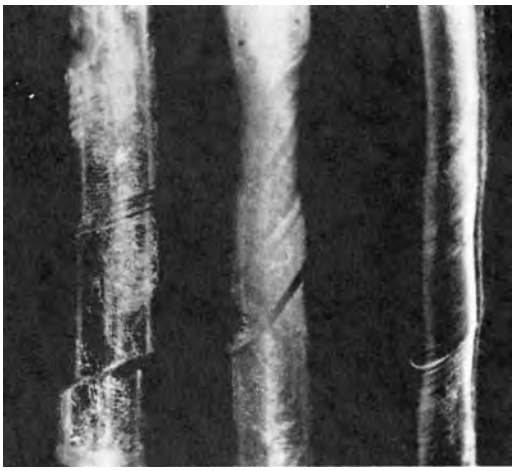


Figure 2 Translational slip in zinc single crystals. (E. R. Parker.)

produce a **stacking fault** such as *ABCABABC*. . . . The result is then a mixture of fcc and hcp stacking.

Deformation by slip is inhomogeneous: large shear displacements occur on a few widely separated slip planes, while parts of the crystal lying between slip planes remain essentially undeformed. A property of slip is the Schmid law of the critical shear stress: slip takes place along a given slip plane and direction when the corresponding *component* of shear stress reaches the critical value.

Slip is one mode of plastic deformation. Another mode, **twinning**, is observed particularly in hcp and bcc structures. During slip a considerable displacement occurs on a few widely separated slip planes. During twinning, a partial displacement occurs successively on each of many neighboring crystallographic planes. After twinning, the deformed part of the crystal is a mirror image of the undeformed part. Although both slip and twinning are caused by the motion of dislocations, we shall be concerned primarily with slip.

DISLOCATIONS

The low observed values of the critical shear stress are explained in terms of the motion through the lattice of a line imperfection known as a dislocation. The idea that slip propagates by the motion of dislocations was published in 1934 independently by Taylor, Orowan, and Polanyi; the concept of dislocations was introduced somewhat earlier by Prandtl and Dehlinger. There are several basic types of dislocations. We first describe an **edge dislocation**. Figure 3 shows a simple cubic crystal in which slip of one atom distance has occurred over the left half of the slip plane but not over the right half. The boundary between the slipped and unslipped regions is called the dislocation. Its position is marked by the termination of an extra vertical half-plane of atoms crowded into

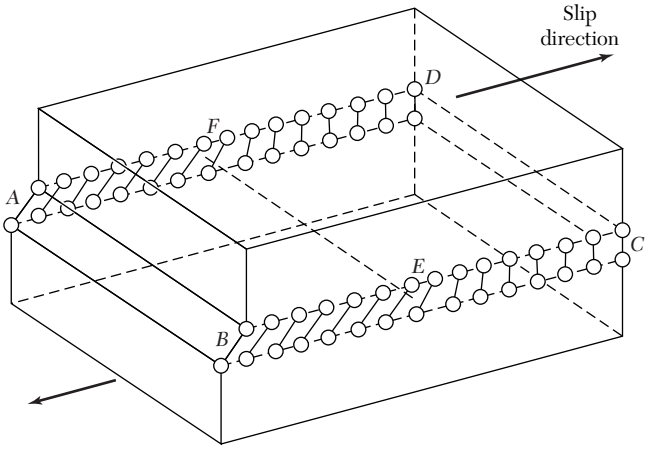


Figure 3 An edge dislocation *EF* in the glide plane *ABCD*. The figure shows the slipped region *ABEF* in which the atoms have been displaced by more than half a lattice constant and the unslipped region *FECD* with displacement less than half a lattice constant.

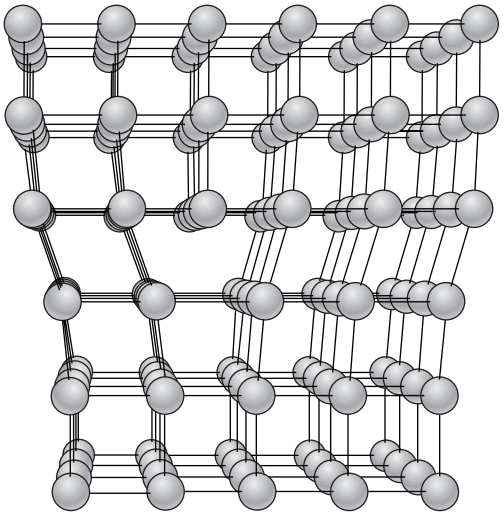


Figure 4 Structure of an edge dislocation. The deformation may be thought of as caused by inserting an extra plane of atoms on the upper half of the y axis. Atoms in the upper half-crystal are compressed by the insertion; those in the lower half are extended.

the upper half of the crystal as shown in Fig. 4. Near the dislocation the crystal is highly strained. The simple edge dislocation extends indefinitely in the slip plane in a direction normal to the slip direction. In Fig. 5 we show a photograph of a dislocation in a two-dimensional soap bubble raft obtained by the method of Bragg and Nye.

The mechanism responsible for the mobility of a dislocation is shown in Fig. 6. The motion of an edge dislocation through a crystal is analogous to the passage of a ruck or wrinkle across a rug: the ruck moves more easily than the whole rug. If atoms on one side of the slip plane are moved with respect to

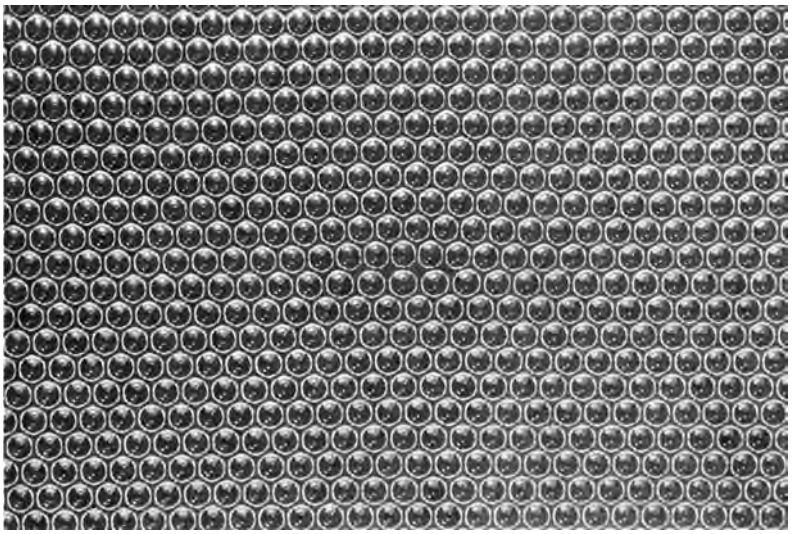


Figure 5 A dislocation in a two-dimensional bubble raft. The dislocation is most easily seen by turning the page by 30° in its plane and sighting at a low angle. (W. M. Lomer, after Bragg and Nye.)

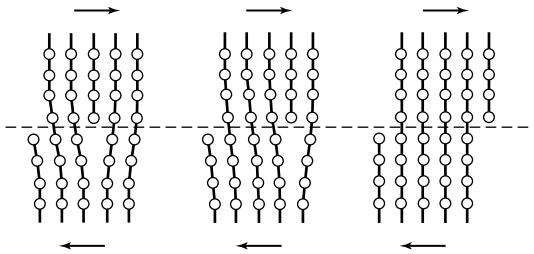


Figure 6 Motion of a dislocation under a shear tending to move the upper surface of the specimen to the right. (D. Hull.)

those on the other side, atoms at the slip plane will experience repulsive forces from some neighbors and attractive forces from others across the slip plane. These forces cancel to a first approximation. The external stress required to move a dislocation has been calculated and is quite small, below 10^5 dyn/cm^2 when the bonding forces in the crystal are not highly directional. Thus dislocations may make a crystal very plastic. Passage of a dislocation through a crystal is equivalent to a slip displacement of one part of the crystal.

The second simple type of dislocation is the **screw dislocation**, sketched in Figs. 7 and 8. A screw dislocation marks the boundary between slipped and unslipped parts of the crystal. The boundary *parallels* the slip direction, instead of lying perpendicular to it as for the edge dislocation. The screw dislocation may be thought of as produced by cutting the crystal partway through with a knife and shearing it parallel to the edge of the cut by one atom spacing. A screw dislocation transforms successive atom planes into the surface of a helix; this accounts for the name of the dislocation.

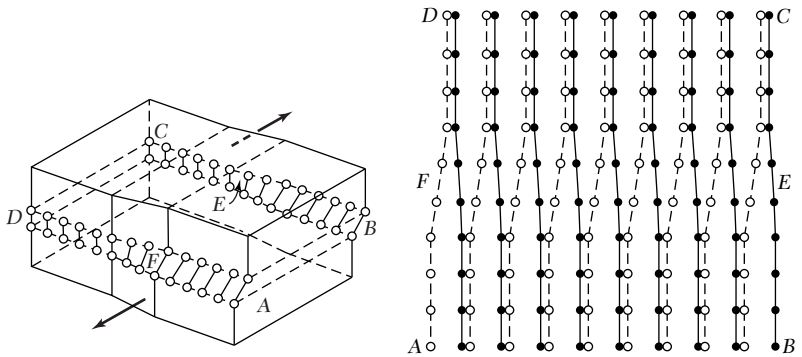


Figure 7 A screw dislocation. A part *ABEF* of the slip plane has slipped in the direction parallel to the dislocation line *EF*. A screw dislocation may be visualized as a helical arrangement of lattice planes, such that we change planes on going completely around the dislocation line. (After Cottrell.)

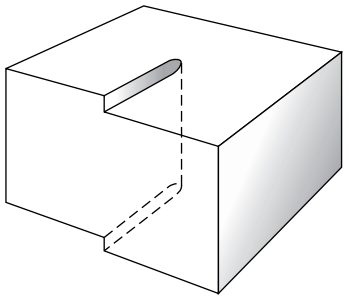


Figure 8 Another view of a screw dislocation. The broken vertical line that marks the dislocation is surrounded by strained material.

Burgers Vectors

Other dislocation forms may be constructed from segments of edge and screw dislocations. Burgers has shown that the most general form of a linear dislocation pattern in a crystal can be described as shown in Fig. 9. We consider any closed curve within a crystal, or an open curve terminating on the surface at both ends: (a) Make a cut along any simple surface bounded by the line. (b) Displace the material on one side of this surface by a vector **b** relative to the other side; here **b** is called the **Burgers vector**. (c) In regions where **b** is not parallel to the cut surface, this relative displacement will either produce a gap or cause the two halves to overlap. In these cases we imagine that we either add material to fill the gap or subtract material to prevent overlap. (d) Rejoin the material on both sides. We leave the strain displacement intact at the time of rewelding, but afterwards we allow the medium to come to internal equilibrium. The resulting strain pattern is that of the dislocation characterized jointly by the boundary curve and the Burgers vector. The Burgers vector must be equal to a lattice vector in order that the rewelding process will maintain the crystallinity of the material. The Burgers vector of a screw dislocation (Figs. 7 and 8) is parallel to the dislocation line; that of an edge dislocation (Figs. 3 and 4) is perpendicular to the dislocation line and lies in the slip plane.

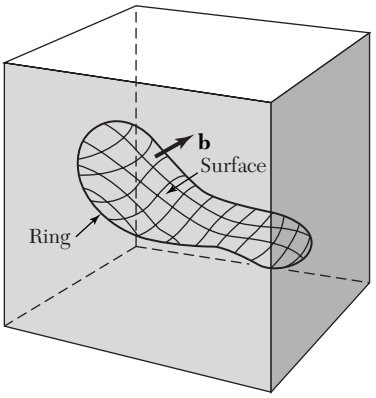


Figure 9 General method of forming a dislocation ring in a medium. The medium is represented by the rectangular block. The ring is represented by the closed curve in the interior in the block. A cut is made along the surface bounded by the curve and indicated by the contoured area. The material on one side of the cut is displaced relative to that on the other by vector distance **b**, which may be oriented arbitrarily relative to the surface. Forces will be required to effect the displacement. The medium is filled in or cut away so as to be continuous after the displacement. It is then joined in the displaced state and the applied forces are relaxed. Here **b** is the Burgers vector of the dislocation. (After Seitz.)

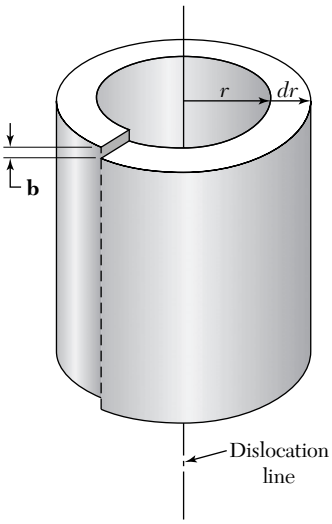


Figure 10 Shell of elastically distorted crystal surrounding screw dislocation with Burgers vector **b**; see also Fig. 16.

Stress Fields of Dislocations

The stress field of a screw dislocation is particularly simple. Figure 10 shows a shell of material surrounding an axial screw dislocation. The shell of circumference $2\pi r$ has been sheared by an amount b to give a shear strain $e = b/2\pi r$. The corresponding shear stress in an elastic continuum is

$$\sigma = Ge = Gb/2\pi r \ . \tag{4}$$

This expression does not hold in the region immediately around the dislocation line, as the strains here are too large for continuum or linear elasticity theory to apply. The elastic energy of the shell is $dE_s = \frac{1}{2}Ge^2\,dV = (Gb^2/4\pi)\,dr/r$ per unit length. The total elastic energy per unit length of a screw dislocation is found on integration to be

$$E_S = \frac{Gb^2}{4\pi}\ln\frac{R}{r_0}\ , \tag{5}$$

where R and r_0 are appropriate upper and lower limits for the variable r. A reasonable value of r_0 is comparable to the magnitude b of the Burgers vector or to the lattice constant; the value of R cannot exceed the dimensions of the crystal. The value of the ratio R/r_0 is not very important because it enters in a logarithm term.

We now show the form of the energy of an edge dislocation. Let σ_{rr} and $\sigma_{\theta\theta}$ denote the tensile stresses in the radial and circumferential directions, and let $\sigma_{r\theta}$ denote the shear stress. In an isotropic elastic continuum, σ_{rr} and $\sigma_{\theta\theta}$ are proportional to $(\sin\theta)/r$: we need a function that falls off as $1/r$ and that changes sign when y is replaced by $-y$. The shear stress $\sigma_{r\theta}$ is proportional to $(\cos\theta)/r$; considering the plane $y = 0$, we see from Fig. 4 that the shear stress is an odd function of x. The constants of proportionality in the stress are proportional to the shear modulus G and to the Burgers vector b of the displacement. The final result is

$$\sigma_{rr} = \sigma_{\theta\theta} = -\frac{Gb}{2\pi(1-\nu)}\frac{\sin\theta}{r}\ , \qquad \sigma_{r\theta} = \frac{Gb}{2\pi(1-\nu)}\frac{\cos\theta}{r}\ , \tag{6}$$

where the Poisson ratio $\nu \approx 0.3$ for most crystals. The strain energy of a unit length of edge dislocation is

$$E_e = \frac{Gb^2}{4\pi(1-\nu)}\ln\frac{R}{r_o}\ . \tag{7}$$

We want an expression for the shear stress component σ_{xy} on planes parallel to the slip plane in Fig. 4. From the stress components σ_{rr}, $\sigma_{\theta\theta}$, and $\sigma_{r\theta}$ evaluated on the plane a distance y above the slip plane, we find

$$\sigma_{xy} = \frac{Gb}{2\pi(1-\nu)}\cdot\frac{x(x^2-y^2)}{(x^2+y^2)^2}\ . \tag{8}$$

It is shown in Problem 3 that the force caused by a resolved uniform shear stress σ is $F = b\sigma$ per unit length of dislocation. The force that an edge dislocation at the origin exerts upon a similar one at the location (y, θ) is

$$F = b\sigma_{xy} = \frac{Gb^2}{2\pi(1-\nu)}\frac{\sin 4\theta}{4y} \tag{9}$$

per unit length. Here F is the component of force in the slip direction.

Low-angle Grain Boundaries

Burgers suggested that low-angle boundaries between adjoining crystallites or crystal grains consist of arrays of dislocations. A simple example of the Burgers model of a grain boundary is shown in Fig. 11. The boundary occupies a (010) plane in a simple cubic lattice and divides two parts of the crystal that have a [001] axis in common. Such a boundary is called a pure tilt boundary: the misorientation can be described by a small rotation θ about the common [001] axis of one part of the crystal relative to the other. The tilt boundary is represented as an array of edge dislocations of spacing $D = b/\theta$, where b is the Burgers vector of the dislocations. Experiments have substantiated this model. Figure 12 shows the distribution of dislocations along small-angle grain boundaries, as observed with an electron microscope. Further, Read and Shockley derived a theory of the interfacial energy as a function of the angle of tilt, with results in excellent agreement with measurements.

Direct verification of the Burgers model is provided by the quantitative x-ray and optical studies of low-angle boundaries in germanium crystals by Vogel

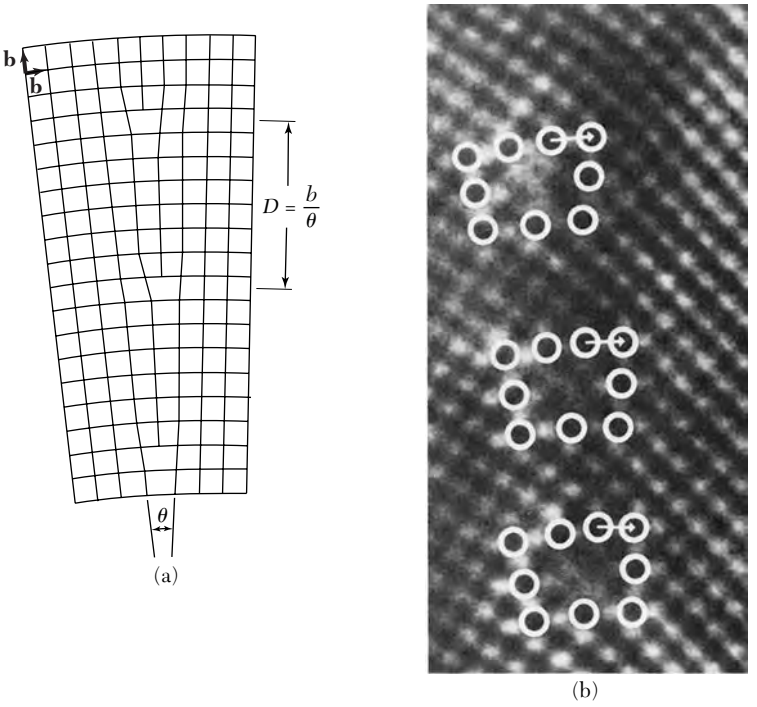


Figure 11 (*a*) Low-angle grain boundary, after Burgers. (*b*) Electron micrograph of a low-angle grain boundary in molybdenum. The three dislocations in the image each have the same Burgers vector as in the drawing in Fig. 11*a*. The white circles mark the positions of atomic columns normal to the plane of the paper. Each array of circles defines the position of a dislocation, with four circles on the top of each array and three circles below. Closure failure is indicated by the arrows which define the Burgers vectors. (Courtesy of R. Gronsky.)

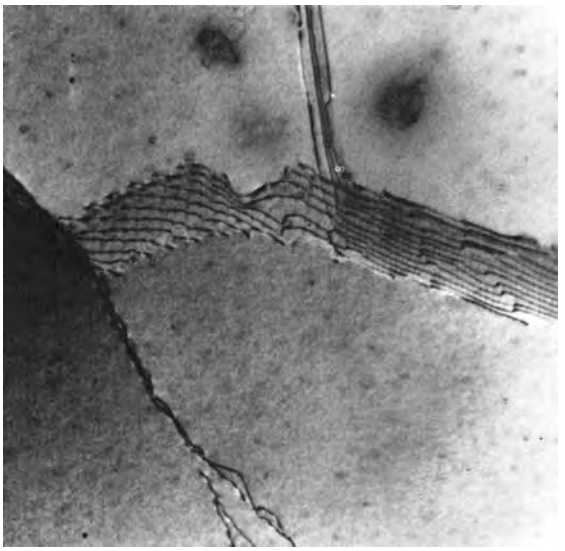


Figure 12 Electron micrograph of dislocation structures in low-angle grain boundaries in an Al-7 percent Mg solid solution. Notice the lines of small dots on the right. Mag. ×17,000. (R. Goodrich and G. Thomas.)

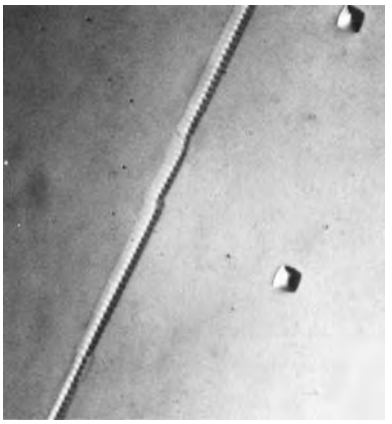


Figure 13 Dislocation etch pits in low-angle boundary on (100) face of germanium; the angle of the boundary is 27.5". The boundary lies in a (011) plane; the line of the dislocations is [100]. The Burgers vector is the shortest lattice translation vector, or $|b| = a/\sqrt{2} = 4.0$ Å. (F. L. Vogel, Jr.)

and co-workers. By counting etch pits along the intersection of a low-angle grain boundary with an etched germanium surface (Fig. 13), they determined the dislocation spacing D. They assumed that each etch pit marked the end of a dislocation. The angle of tilt calculated from the relation $\theta = b/D$ agrees well with the angle measured directly by means of x-rays.

The interpretation of low-angle boundaries as arrays of dislocations is further supported by the fact that pure tilt boundaries move normal to themselves on application of a suitable stress. The motion has been demonstrated in

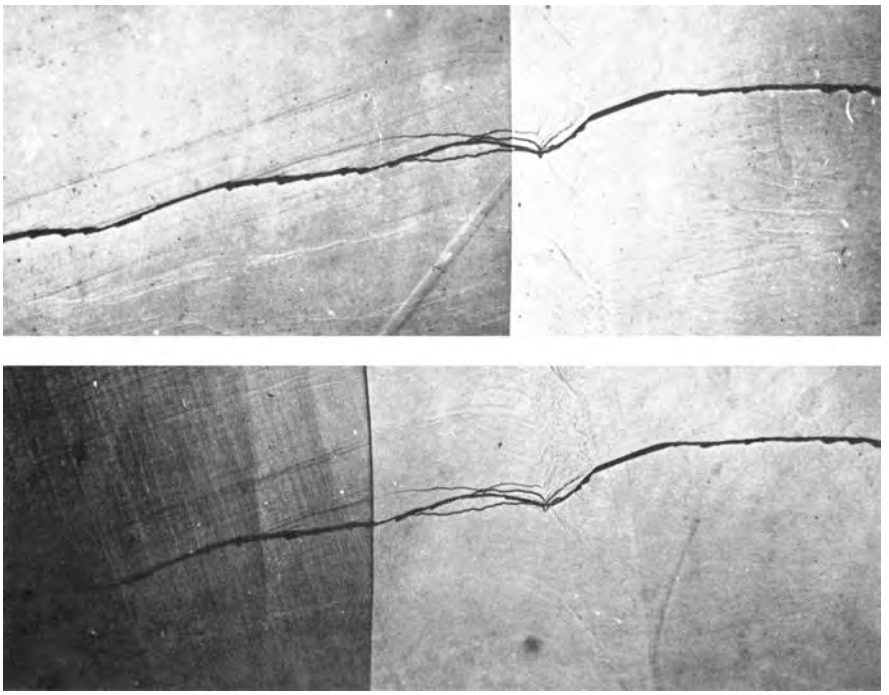


Figure 14 Motion of a low-angle grain boundary under stress. The boundary is the straight vertical line, and it is photographed under vertical illumination, thereby making evident the 2° angular change in the cleavage surface of the zinc crystal at the boundary. The irregular horizontal line is a small step in the cleavage surface which serves as a reference mark. The crystal is clamped at the left; at the right it is subject to a force normal to the plane of the page. *Top,* original position of boundary; *bottom,* moved back 0.4 mm. (J. Washburn and E. R. Parker.)

a beautiful experiment, Fig. 14. The specimen is a bicrystal of zinc containing a 2° tilt boundary with dislocations about 30 atomic planes apart. One side of the crystal was clamped, and a force was applied at a point on the opposite side of the boundary. Motion of the boundary took place by cooperative motion of the dislocations in the array, each dislocation moving an equal distance in its own slip plane. The motion was produced by stresses of the order of magnitude of the yield stress for zinc crystals, strong evidence that ordinary deformation results from the motion of dislocations.

Grain boundaries and dislocations offer relatively little resistance to diffusion of atoms in comparison with diffusion in perfect crystals. A dislocation is an open passage for diffusion. Diffusion is greater in plastically deformed material than in annealed crystals. Diffusion along grain boundaries controls the rates of some precipitation reactions in solids: the precipitation of tin from lead-tin solutions at room temperature proceeds about 10^8 times faster than expected from diffusion in an ideal lattice.

Dislocation Densities

The density of dislocations is the number of dislocation lines that intersect a unit area in the crystal. The density ranges from well below 10^2 dislocations/cm^2 in the best germanium and silicon crystals to 10^{11} or 10^{12} dislocations/cm^2 in heavily deformed metal crystals. The methods available for estimating dislocation densities are compared in Table 2. The actual dislocation configurations in cast or annealed (slowly cooled) crystals correspond either to a group of low-angle grain boundaries or to a three-dimensional network of dislocations arranged in cells, as shown in Fig. 15.

Lattice vacancies that precipitate along an existing edge dislocation will eat away a portion of the extra half-plane of atoms and cause the dislocation to climb, which means to move at right angles to the slip direction. If no dislocations are

Table 2 Methods for estimating dislocation densities[a]

Technique	Specimen thickness	Width of image	Maximum practical density, per cm^2
Electron microscopy	>1000 Å	~100 Å	$10^{11}-10^{12}$
X-ray transmission	0.1–1.0 mm	5 μm	10^4-10^5
X-ray reflection	<2 μm (min.) – 50 μm (max.)	2 μm	10^6-10^7
Decoration	~10 μm (depth of focus)	0.5 μm	2×10^7
Etch pits	no limit	0.5 μm[b]	4×10^8

[a]W. G. Johnston.
[b]Limit of resolution of etch pits.

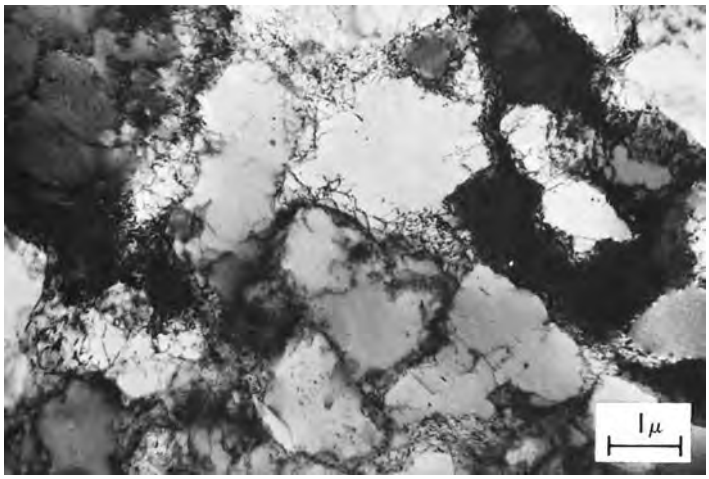


Figure 15 Cell structure of three-dimensional tangles of dislocations in deformed aluminum. (P. R. Swann.)

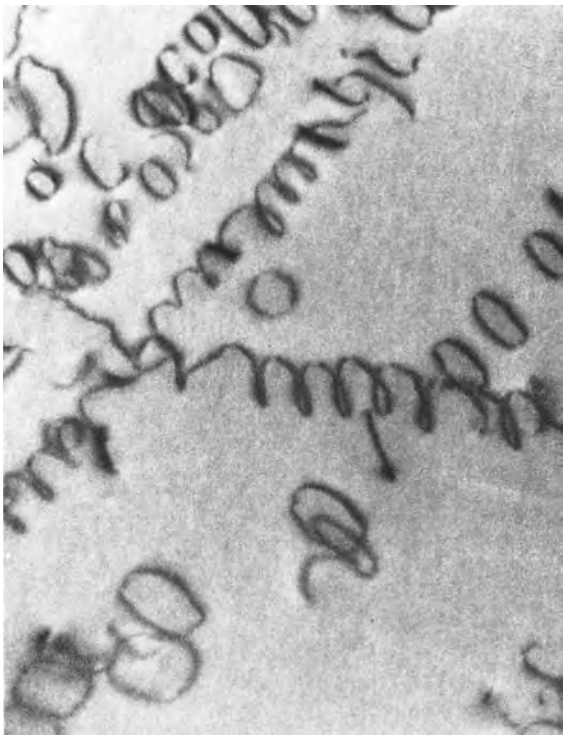


Figure 16 Electron micrograph of dislocation loops formed by aggregation and collapse of vacancies in Al–5 percent Mg quenched from 550°C. The helical dislocations are formed by vacancy condensation on a screw dislocation. Mag. ×43,000. (A. Eikum and G. Thomas.)

present, the crystal will become supersaturated with lattice vacancies; their precipitation in cylindrical vacancy plates may be followed by collapse of the plates and formation of dislocation rings that grow with further vacancy precipitation, as in Fig. 16.

Dislocation Multiplication and Slip

Plastic deformation causes a very great increase in dislocation density, typically from 10^8 to about 10^{11} dislocations/cm^2 during deformation. If a dislocation moves completely across its slip plane, an offset of one atom spacing is produced, but offsets up to 100 to 1000 atom spacings are observed. This means that dislocations multiply during deformation.

Consider a closed circular dislocation loop of radius r surrounding a slipped area having the radius of the loop. Such a loop will be partly edge, partly screw, and mostly of intermediate character. The strain energy of the loop increases as its circumference, so that the loop will tend to shrink in size. However, the loop will tend to expand if a shear stress is acting that favors slip.

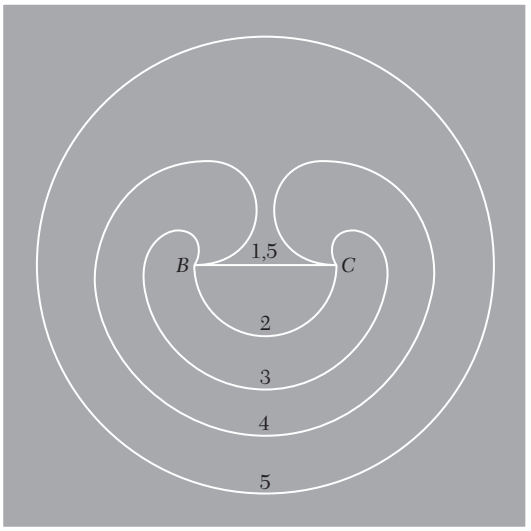


Figure 17 Frank-Read mechanism for multiplication of dislocations, showing successive stages in the generation of a dislocation loop by the segment *BC* of a dislocation line. The process can be repeated indefinitely.

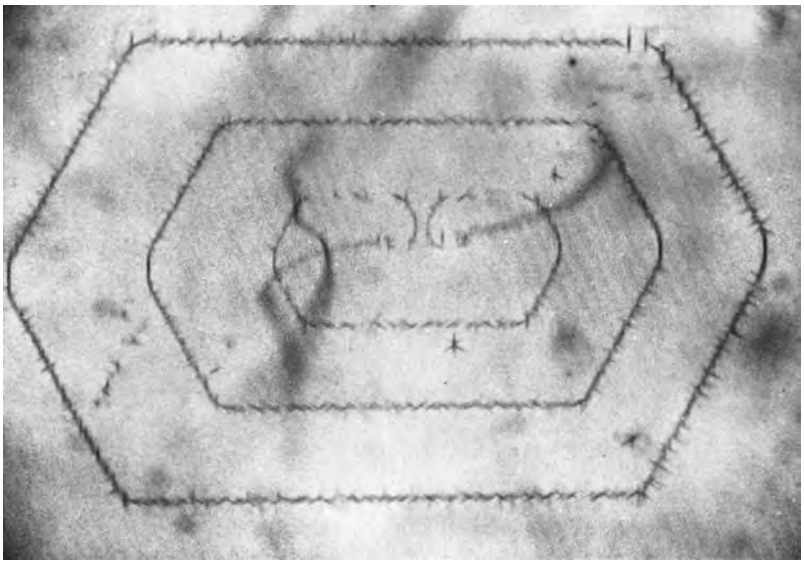


Figure 18 A Frank-Read dislocation source in silicon, decorated with copper precipitates and viewed with infrared illumination. Two complete dislocation loops are visible, and the third, innermost loop is near completion. (After W. C. Dash.)

A common feature of all dislocation sources is the bowing of dislocations. A dislocation segment pinned at each end is called a **Frank-Read source**, and it can lead (Fig. 17) to the generation of a large number of concentric dislocations on a single slip plane (Fig. 18). Related types of dislocation multiplication mechanisms account for slip and for the increased density of dislocations during plastic deformation. Double cross-slip is the most common source.

STRENGTH OF ALLOYS

Pure crystals are very plastic and yield at very low stresses. There appear to be four important ways of increasing the yield strength of an alloy so that it will withstand shear stresses as high as 10^{-2} G. They are mechanical blocking of dislocation motion, pinning of dislocations by solute atoms, impeding dislocation motion by short-range order, and increasing the dislocation density so that tangling of dislocations results. All four strengthening mechanisms depend for their success upon impeding dislocation motion. A fifth mechanism, that of removing all dislocations from the crystal, may operate for certain fine hairlike crystals (whiskers) that are discussed in the section on crystal growth.

Mechanical blocking of dislocation motion can be produced most directly by introducing tiny particles of a second phase into a crystal lattice. This process is followed in the hardening of steel, where particles of iron carbide are precipitated into iron, and in hardening aluminum, where particles of Al_2Cu are precipitated. The pinning of a dislocation by particles is shown in Fig. 19.

In strengthening by the addition of small particles there are two cases to be considered: either the particle can be deformed with the matrix, which requires that the particle can be traversed by the dislocation, or the particle cannot be traversed by the dislocation. If the particle cannot be cut, the stress

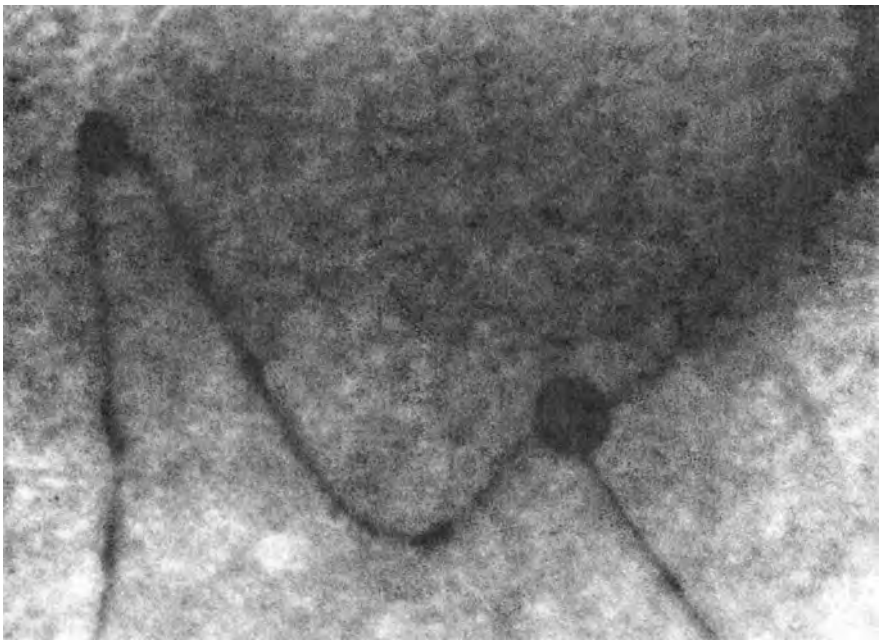


Figure 19 Dislocations pinned by particles in magnesium oxide. (Electron micrograph by G. Thomas and J. Washburn.)

necessary to force a dislocation between particles spaced L apart on a slip plane should be approximately

$$\sigma/G = b/L \ . \tag{10}$$

The smaller the spacing L, the higher is the yield stress σ. Before particles precipitate, L is large and the strength is low. Immediately after precipitation is complete and many small particles are present, L is a minimum and the strength is a maximum. If the alloy is then held at a high temperature, some particles grow at the expense of others, so that L increases and the strength drops. Hard intermetallic phases, such as refractory oxides, cannot be cut by dislocations.

The strength of dilute solid solutions is believed to result from the pinning of dislocations by solute atoms. The solubility of a foreign atom will be greater in the neighborhood of a dislocation than elsewhere in a crystal. An atom that tends to expand the crystal will dissolve preferentially in the expanded region near an edge dislocation. A small atom will tend to dissolve preferentially in the contracted region near the dislocation—a dislocation offers both expanded and contracted regions.

As a result of the affinity of solute atoms for dislocations, each dislocation will collect a cloud of associated solute atoms during cooling, at a time when the mobility of solute atoms is high. At still lower temperatures, diffusion of solute atoms effectively ceases, and the solute atom cloud becomes fixed in the crystal. When a dislocation moves, leaving its solute cloud behind, the energy of the crystal must increase. The increase in energy can only be provided by an increased stress acting on the dislocation as it pulls away from the solute atom cloud, and so the presence of the cloud strengthens the crystal.

The passage of a dislocation across a slip plane in pure crystals does not alter the binding energy across the plane after the dislocation is gone. The internal energy of the crystal remains unaffected. The same is true for random solid solutions, because the solution is equally random across a slip plane after slip. Most solid solutions, however, have short-range order. Atoms of different species are not arranged at random on the lattice sites, but tend to have an excess or a deficiency of pairs of unlike atoms. Thus in ordered alloys dislocations tend to move in pairs: the second dislocation reorders the local disorder left by the first dislocation.

The strength of a crystalline material increases with plastic deformation. The phenomenon is called **work-hardening** or **strain-hardening**. The strength is believed to increase because of the increased density of dislocations and the greater difficulty of moving a given dislocation across a slip plane that is threaded by many dislocations. Strain-hardening frequently is employed in the strengthening of materials, but its usefulness is limited to low enough temperatures so that annealing does not occur.

An important factor in strain-hardening is the total density of dislocations. In most metals dislocations tend to form cells (Fig. 15) of dislocation-free

areas of dimensions of the order of 1 μm. But unless we can get a uniform high density of dislocations we cannot strain-harden a metal to its theoretical strength, because of slip in the dislocation-free areas. A high total density is accomplished by explosive deformation or by special thermal-mechanical treatments, as of martensite in steel.

Each of the mechanisms of strengthening crystals can raise the yield strength to the range of 10^{-3} G to 10^{-2} G. All mechanisms begin to break down at temperatures where diffusion can occur at an appreciable rate. When diffusion is rapid, precipitated particles dissolve; solute clouds drift along with dislocations as they glide; short-range order repairs itself behind slowly moving dislocations; and dislocation climb and annealing tend to decrease the dislocation density. The resulting time-dependent deformation is called creep. This irreversible motion precedes the elastic limit. The search for alloys for use at very high temperatures is a search for reduced diffusion rates, so that the four strengthening mechanisms will survive to high temperatures. But the central problem of strong alloys is not strength, but ductility, for failure is often by fracture.

DISLOCATIONS AND CRYSTAL GROWTH

In some cases the presence of dislocations may be the controlling factor in crystal growth. When crystals are grown in conditions of low supersaturation, of the order of 1 percent, it has been observed that the growth rate is enormously faster than that calculated for an ideal crystal. The actual growth rate is explained in terms of the effect of dislocations on growth.

The theory of growth of ideal crystals predicts that in crystal growth from vapor, a supersaturation (pressure/equilibrium vapor pressure) of the order of 10 is required to nucleate new crystals, of the order of 5 to form liquid drops, and of 1.5 to form a two-dimensional monolayer of molecules on the face of a perfect crystal. Volmer and Schultze observed growth of iodine crystals at vapor supersaturations down to less than 1 percent, where the growth rate should have been down by the factor $\exp(-3000)$ from the rate defined as the minimum observable growth.

The large disagreement expresses the difficulty of nucleating a new monolayer on a completed surface of an ideal crystal. But if a screw dislocation is present (Fig. 20), it is never necessary to nucleate a new layer: the crystal will grow in spiral fashion at the *edge* of the discontinuity shown. An atom can be bound to a step more strongly than to a plane. The calculated growth rates for this mechanism are in good agreement with observation. We expect that nearly all crystals in nature grown at low supersaturation will contain dislocations, as otherwise they could not have grown. Spiral growth patterns have been observed on a large number of crystals. A beautiful example of the growth pattern from a single screw dislocation is given in Fig. 21.

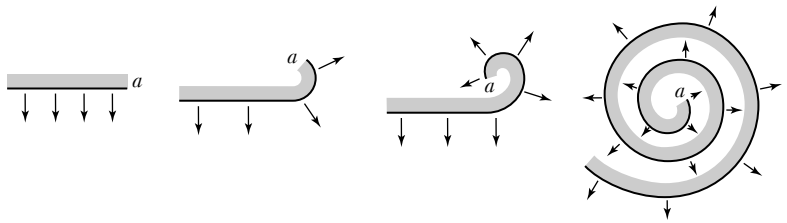


Figure 20 Development of a spiral step produced by intersection of a screw dislocation with the surface of a crystal as in Fig. 8. (F. C. Frank.)

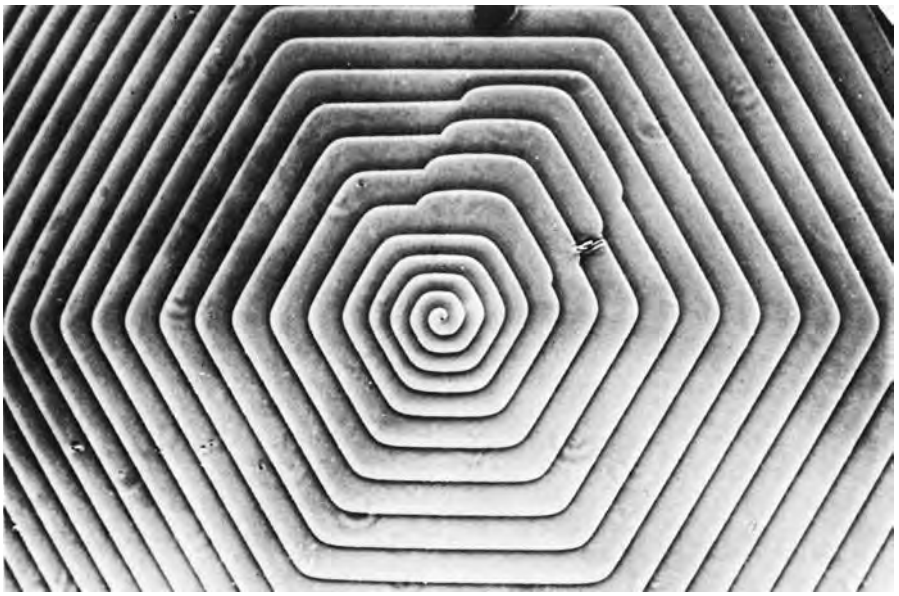


Figure 21 Phase contrast micrograph of a hexagonal spiral growth pattern on a SiC crystal. The step height is 165 Å. (A. R. Verma.)

If the growth rate is independent of direction of the edge in the plane of the surface, the growth pattern is an Archimedes spiral, $r = a\theta$, where a is a constant. The limiting minimum radius of curvature near the dislocation is determined by the supersaturation. If the radius of curvature is too small, atoms on the curved edge evaporate until the equilibrium curvature is attained. Away from the origin each part of the step acquires new atoms at a constant rate, so that $dr/dt = \text{const}$.

Whiskers

Fine hairlike crystals, or **whiskers**, have been observed to grow under conditions of high supersaturation without the necessity for more than perhaps one dislocation. It may be that these crystals contain a single axial screw dislocation

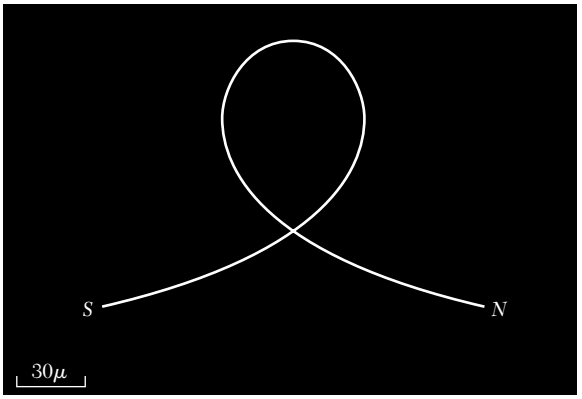


Figure 22 A nickel whisker of diameter 1000 Å bent in a loop. (R. W. De Blois.)

that aids their essentially one-dimensional growth. From the absence of dislocations we would expect these crystal whiskers to have high yield strengths, of the order of the calculated value $G/30$ discussed earlier in this chapter. A single axial screw dislocation, if present, could not cause yielding, because in bending the crystal the dislocation is not subjected to a shear stress parallel to its Burgers vector. That is, the stress is not in a direction that can cause slip. Herring and Galt observed whiskers of tin of radius $\sim 10^{-4}$ cm with elastic properties near those expected from theoretically perfect crystals. They observed yield strains of the order of 10^{-2}, which correspond to shear stresses of order $10^{-2}\,G$, about 1000 times greater than in bulk tin, confirming the early estimates of the strength of perfect crystals. Theoretical or ideal elastic properties have been observed for a number of materials as for carbon nanotubes. A single domain whisker of nickel is shown in Fig. 22.

HARDNESS OF MATERIALS

The hardness of materials is measured in several ways, the simplest test for nonmetals being the scratch test. Substance A is harder than substance B if A will scratch B but B will not scratch A. A standard scale is used for representative minerals, with diamond, the hardest, assigned the value 10 and talc, the softest, assigned the value 1:

10 diamond C	5 apatite $Ca_5(PO_4)_3F$
9 corundum Al_2O_3	4 fluorite CaF_2
8 topaz $Al_2SiO_4F_2$	3 calcite $CaCO_3$
7 quartz SiO_2	2 gypsum $CaSO_4 \cdot 2H_2O$
6 orthoclase $KAlSi_3O_8$	1 talc $3MgO \cdot 4SiO_2 \cdot H_2O$

There is great current interest in the development of materials of great hardness, for example as films for use as scratch-resistant coatings on lenses.